Kinetics and Catalysis, Vol. 46, No. 3, 2005, pp. 387–395. Translated from Kinetika i Kataliz, Vol. 46, No. 3, 2005, pp. 414–422.

Mechanism of the Formation of O_2^- Radical Anions on CeO_2 and (0.5–10)% CeO_2/ZrO_2 during the Adsorption of an NO–O_2 Mixture

A. N. Il'ichev, M. D. Shibanova, A. A. Ukharskii, A. M. Kuli-zade, and V. N. Korchak

Semenov Institute of Chemical Physics, Russian Academy of Sciences, Moscow, 119991 Russia

Received November 11, 2003

Abstract—It is established by ESR that the adsorption of an NO + O_2 mixture at 20°C on oxidized CeO_2 (O_2, T = 400–700°C) produces radical anions O_2^- located both on isolated Ce^{4+} cations (O_2^-(1)) and in associated anionic vacancies (O_2^-(2)). These species differ in thermal stability. For example, O_2^-(2) decomposes at 20°C, while O_2^-(1) decomposes at 50°C. Only O_2^- (1) species are observed at –196°C in ZrO_2-supported CeO_2. In the case of NO + O_2 adsorption at 20°C, O_2^- is stabilized on Zr^{4+} cations and decomposes at 270°C. Increasing the cerium oxide content of the ZrO_2 surface from 0.5 to 10% only partially inhibits the formation of O_2^-–Zr^{4+}. The Zr^{4+} cation is shown to possess a higher Lewis acidity than the Ce^{4+} cation, and the ionic bond in O_2^-–Zr^{4+} complexes is stronger than that in O_2^-–Ce^{4+} complexes. ESR, temperature-programmed desorption, and IR spectroscopic data for various adsorption complexes of NO on CeO_2 suggest that, in the key step of O_2^- formation, free electrons appear on the surface owing to the conversion of adsorbed NO molecules into nitrito chelates on coordinately unsaturated ion pairs Ce^{4+}–O_2^-.

INTRODUCTION

Catalytic systems containing CeO_2, ZrO_2, and CeO_2–ZrO_2 are promising for heterogeneous neutralization of nitrogen oxides NO_x (NO and NO_2) and oxidation of hydrocarbons and CO in automobile and plant exhaust. It is assumed that CeO_2 in these catalysts exerts its promoting effect through supply of O_2 to the reaction [1–3]. ZrO_2 improves the thermal stability of the catalyst and the redox properties of CeO_2 [4, 5]. It has recently been shown [6] that CeO_2 and CeO_2–ZrO_2 are active in the selective catalytic reduction of NO_x with hydrocarbons in excess oxygen, but their role in the reactions is poorly understood.

Electron transfer between adsorbed reactants can play a significant role in NO_x reduction [7]. Study of this process on MgO showed that the coadsorption of oxygen and hydrogen or weak acids (H–X) [8–12] is accompanied by the formation of O_2^- radical anions. In these reactions, the first step is the dissociative adsorption of H–X (X–H + $O_{surf}^{2-} \longrightarrow X^- + OH^-$) and the second step is electron transfer ($X^- + O_2 \longrightarrow X^+ + O_2^-$). Earlier, we studied the coadsorption of O_2 with NO and NO_2 on ZrO_2 and found that adsorbed nitrogen oxides also initiate the formation of O_2^- on ZrO_2 [13]. The reaction mechanism proposed in [14] assumes that free electrons are formed during the formation of NO_2^- and NO_3^- ions through the adsorption of nitrogen oxides on M^{n+}–O^{2-} ion pairs.

To confirm the above view of the mechanism of O_2^- formation during the adsorption of an NO + O_2 mixture (O_2^-(NO + O_2)), we studied this reaction on pure CeO_2 and on (0.5–10)%CeO_2/ZrO_2 samples, varying thermal oxidation condition for the catalysts. NO adsorption species and their interaction with oxygen on CeO_2 were also studied by ESR, temperature-programmed desorption (TPD), and IR spectroscopy.

EXPERIMENTAL

Cerium and zirconium oxides with a specific surface area of S_{sp} = 50 m^2/g were obtained by decomposition of $Ce(NO_3)_4 \cdot 6H_2O$ and $ZrO(NO_3)_2$ in air at 500°C for 2 h. The specific surface area was determined by the BET method from low-temperature argon adsorption data.

CeO_2/ZrO_2 samples were prepared by impregnating ZrO_2 with cerium nitrate solutions with different salt concentrations (towards a CeO_2 content of (0.5–10) mol %) followed by drying at 100°C and calcination at 350°C in air for 5 h. On the assumption that supported cerium ions are uniformly distributed over the ZrO_2 surface in the (0.5–10)%CeO_2/ZrO_2 samples, the ratio of the

0023-1584/05/4603-0387 © 2005 MAIK "Nauka/Interperiodica"

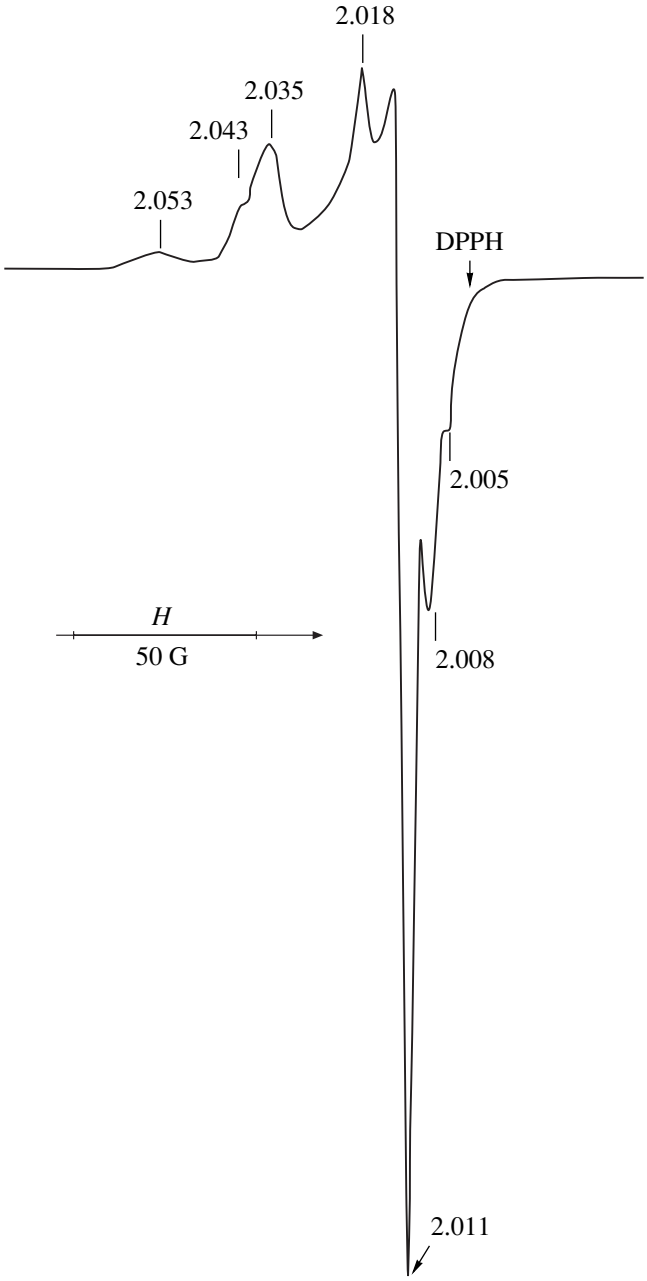

Fig. 1. ESR spectrum of $CeO_2(O_2, 400°C)$ after $NO + O_2$ adsorption at $T = 20°C$. The spectrum is recorded at –196°C in vacuum.

number of cerium ions to the number of surface zirconium ions is from 0.15 to 3.

The formation of $O_2^-(NO + O_2)$ was studied by ESR. A 50-mg sample was placed in an ESR tube, pumped to 10^{-4} Pa, heated in vacuum at a prescribed temperature for 1 h, and oxidized in O_2 ($P_{O_2} = 10^2$ Pa) or reduced in H_2 ($P_{H_2} = 10^3$ Pa) at this temperature for 20 min. Next, the sample was cooled to 20°C, pumped, and exposed to the gas. After adsorption, ESR spectra of adsorption complexes were recorded at 20 or –196°C in the X range on an EPR-V spectrometer with a Diapazon temperature attachment. The number of paramagnetic species was determined from twice-integrated ESR spectra using $CuSO_4 \cdot 5H_2O$ as the standard. The accuracy of these measurements was 20%.

Thermal desorption was measured for a sample placed in an ESR tube. The sample was preoxidized at 600°C, and the gas was adsorbed on the sample at 20°C for 5 min. After adsorption, the sample was pumped for 10 min at room temperature and heated at a rate of 10 K/min under continuous pumping. Thermal desorption spectra as temperature dependences of the variation of desorbed gas pressure (w_P) were recorded using a Pirani gage [15]. The composition of the desorbed gas was monitored using an MX-7304 mass spectrometer. The amount of gas desorbed was determined as the change in pressure by extra TPD runs in a closed reactor.

Diffuse reflectance IR spectra were recorded on a Perkin-Elmer RX FT-IR spectrophotometer after 64 scans. For this purpose, a CeO_2 powder (100 mg) was placed in a quartz vacuum cell with CaF_2 windows. The sample was heat-treated in the same way as in the TPD runs.

NO, H_2, and O_2 gases were obtained in vacuum using standard procedures [16].

RESULTS

ESR Data

Formation of O_2^- during adsorption of an NO + O_2 mixture on oxidized CeO_2. No ESR signal is observed upon the adsorption of NO or O_2 (P_{O_2} = 10^2 Pa, P_{NO} = 10 Pa, and T = 20°C) on oxidized $CeO_2(O_2, 400–700°C)$. An ESR signal appears after NO and then O_2 or their mixture NO + O_2 is admitted to the sample. The ESR spectrum recorded at –196°C for $CeO_2(O_2, 400°C)$ after NO + O_2 adsorption is presented in Fig. 1. This spectrum is similar to the spectrum of O_2^- formed on the reduced $CeO_2(H_2, 400°C)$ sample upon oxygen adsorption. Therefore, the adsorption of an NO + O_2 mixture on oxidized CeO_2 produces radical anions O_2^-. The ESR spectra of O_2^- on reduced CeO_2 after O_2 adsorption were studied in detail [17]. Comparison of these spectra with the spectrum shown in Fig. 1 suggests that the line with $g_1 = 2.035$ and $g_2 = 2.011$ and the line with $g_1 = 2.035$, $g_2 = 2.018$, and $g_3 = 2.011$ are due to O_2^- located on Ce^{4+} cations in isolated anionic vacancies ($O_2^-(1)$). The line with $g_1 = 2.053$, $g_2 = 2.008$, and $g_3 = 2.005$ and the line with $g_1 = 2.043$, $g_2 = 2.011$, and $g_3 = 2.008$ can be assigned to O_2^- on Ce^{4+} cations belonging to aggregated anionic vacancies ($O_2^-(2)$).

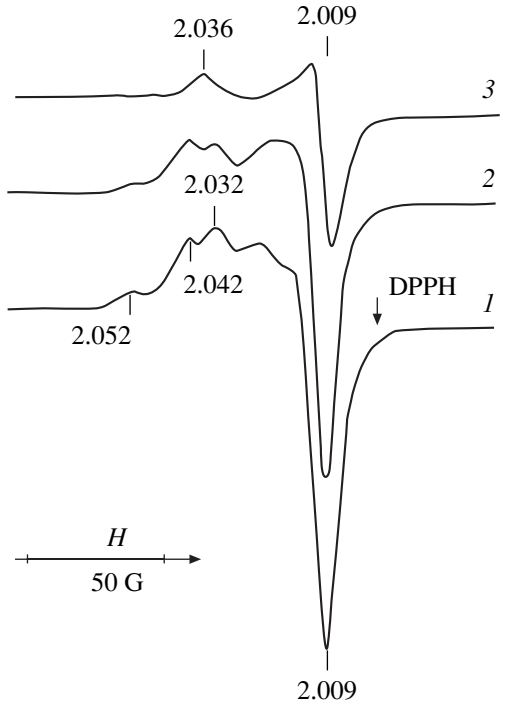

Fig. 2. ESR spectra of $CeO_2(O_2, 400°C)$ after (*1*) admission of an NO + O_2 mixture and (*2*, *3*) subsequent pumping for (*2*) 10 and (*3*) 30 min at T = 20°C. The spectra are recorded at 20°C.

The ESR spectrum of $O_2^-(NO + O_2)$ at 20°C is presented in Fig. 2 (curve *1*). Spectrum *1* contains lines from $O_2^-(1)$ and $O_2^-(2)$. The spectral lines are well resolved in the region of g_1 values and overlap strongly in the region of g_2 and g_3. As the sample is pumped, $O_2^-(1)$ and $O_2^-(2)$ species decompose at different rates (curves *1*–*3*). After the sample is evacuated for 30 min, spectrum *1* transforms into spectrum *3*, which corresponds to $O_2^-(1)$. This species decomposes upon heating at 50°C in vacuum for 10 min. Thus, $O_2^-(2)$ is less stable than $O_2^-(1)$.

As the CeO_2 oxidation temperature is raised from 400 to 700°C, the ratio of $O_2^-(1)$ to $O_2^-(2)$ remains virtually invariable and, as can be seen in Fig. 3 (curve *1*), the total amount of these species increases from 1.3×10^{16} to 3×10^{16} m^{-2} in the temperature range 400–600°C and then decreases to 2×10^{16} m^{-2} at 700°C. The decrease in the amount of O_2^- on $CeO_2(O_2, 700°C)$ is likely to be caused by agglomeration taking place on the sample surface.

In Fig. 3, we plot the concentration of O_2^- on the reduced CeO_2 surface after oxygen adsorption ($P = 1 \times 10^2$ Pa, T = 20°C) versus the temperature at which the oxidized sample has been reduced in hydrogen or vacuum. In the case of hydrogen reduction (curve *2*),

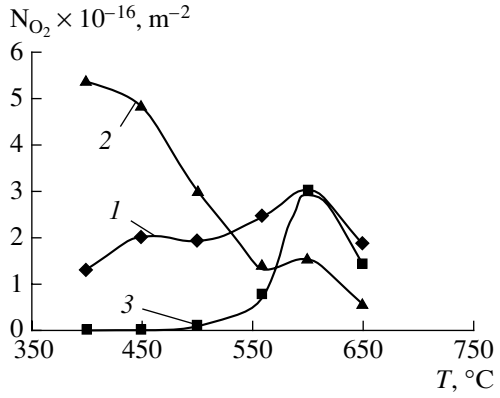

Fig. 3. Amount of O_2^- formed (*1*) upon NO + O_2 adsorption on oxidized CeO_2 and (*2*, *3*) upon O_2 adsorption on CeO_2 that has been reduced in (*2*) hydrogen and (*3*) vacuum versus oxidation or reduction temperature.

the amount of O_2^- decreases monotonically from ~6×10^{16} to 6×10^{15} m^{-2} as the temperature is increased from 400 to 650°C. In the case of heat treatment in vacuum (curve *3*), O_2^- appears on CeO_2 starting at a heat-treatment temperature $T > 470$°C.

Formation of $O_2^-(NO + O_2)$ on oxidized (0.5–10)% CeO_2/ZrO_2. No ESR signal is observed upon the adsorption of O_2 or NO (P_{NO} = 10 Pa, P_{O_2} = 50 Pa, T = 20°C) on (0.5–10)%$CeO_2/ZrO_2(O_2$, 400–700°C) samples. However, a signal appears when an NO + O_2 mixture is adsorbed. This signal can be seen in the spectrum of the 2%$CeO_2/ZrO_2(O_2$, 400°C) sample (Fig. 4, curve *1*). It is characterized by the following components of the g tensor: g_1 = 2.033, g_2 = 2.007, and g_3 = 2.003. Spectrum *1* remains unchanged upon 1-h pumping and is not observed after the sample is heated at 270°C for 10 min. The above g values and high thermal stability are characteristic of O_2^- radical anions formed on Zr^{4+} cations (O_2^-–Zr^{4+}) upon the adsorption of an NO + O_2 mixture on ZrO_2 [14].

An increase in the cerium oxide content of the catalyst from 2 to 10% gives rise to a low-intensity absorption line with g = 2.011 (Fig. 4, curve *2*) against the background of the intense signal of O_2^-–Zr^{4+} in the ESR spectrum of O_2^-. This line can be attributed to the small amount of O_2^- radical anions adsorbed on Ce^{4+} cations.

The plots of $O_2^-(NO + O_2)$ concentration versus the cerium oxide content of the sample for different oxidation temperatures are presented in Fig. 5. As the cerium oxide content is raised from 0.5 to 2%, the O_2^- concentration decreases from 2.8×10^{16} to $(0.5–1.0) \times 10^{16}$ m^{-2}, regardless of the oxidation temperature. The O_2^- con-

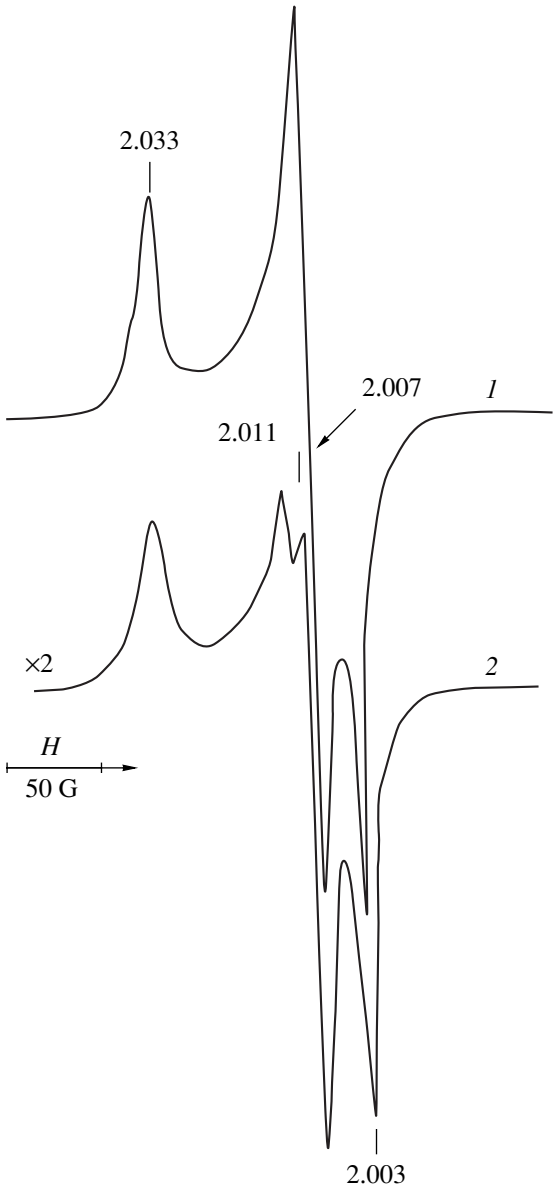

Fig. 4. ESR spectra of $CeO_2/ZrO_2(O_2, 500°C)$ samples with a CeO_2 content of (*1*) 2 and (*2*) 10% after NO + O_2 adsorption and pumping at 20°C.

centration remains in the $(0.5–1.0) \times 10^{16}$ m^{-2} interval as the CeO_2 content is further increased in the range 5–10%.

Thus, in the oxidized (0.5–10)%CeO_2/ZrO_2 samples at 20°C, O_2^-(NO + O_2) radical anions are mainly stabilized in the coordination sphere of Zr^{4+} cations. Supported CeO_2 partially inhibits the formation of O_2^-(NO + O_2) on ZrO_2.

Paramagnetic NO adsorption species and its interaction with O_2 on CeO_2 and CeO_2/ZrO_2. The ESR spectrum of NO adsorbed on $CeO_2(O_2, 300°C)$ at –196°C ($N_{ads} = 6 \times 10^{19}$ molecule/g) is presented in

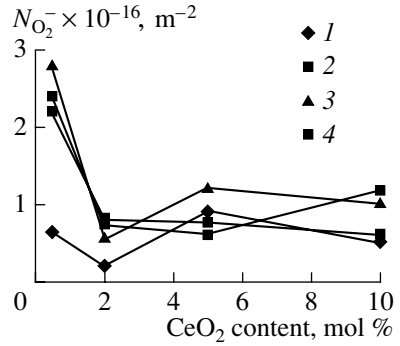

Fig. 5. Amount of O_2^- on CeO_2/ZrO_2 oxidized at (*1*) 400, (*2*) 500, (*3*) 600, and (*4*) 700°C versus the percentage of supported CeO_2.

Fig. 6 (curve *1*). The signal is axially symmetric, with a hyperfine structure due to the interaction between the unpaired electron and the nuclear spin of nitrogen in the NO molecule. The parameters of the *g* and *A* tensors for spectrum *1* are $g_\perp = 1.998$, $g_\parallel = 1.865$, $A_\perp = 30$ G, and $A_\parallel = 0$, which are similar to earlier reported data [18, 19]. The concentration of NO molecules calculated from spectrum *1* is 0.2×10^{17} m^{-2}. Raising the CeO_2 preoxidation temperature from 300 to 600°C increases the NO concentration from 0.2×10^{17} to 7.0×10^{17} m^{-2} (in this case, the parameters of the *g* and *A* tensors remain unchanged), indicating an increase in the concentration of Ce^{4+} Lewis acid sites on which NO molecules are adsorbed [20]. The difference between the concentration of adsorbed NO (1.6×10^{18} m^{-2}) and the NO concentration deduced from ESR data (7.0×10^{17} m^{-2}) is, most likely, due to the formation of nonparamagnetic dimeric NO adsorption species on the surface.

Figure 6 also shows the ESR spectra of NO adsorbed on 10%$CeO_2/ZrO_2(O_2, 500°C)$ (curve *2*) and $ZrO_2(O_2, 500°C)$ (curve *3*) recorded under similar conditions. Spectrum *2* has the same hyperfine structure as spectrum *1*. When the cerium content of the samples is decreased, the hyperfine structure disappears and spectrum *2* transforms into spectrum *3*. It is most likely that spectrum *2* is complicated and is the sum of the ESR spectra of NO adsorbed on Ce^{4+} and Zr^{4+} cations. Spectrum *3* is due to NO molecules adsorbed on Zr^{4+} cations.

The absence of a hyperfine structure in spectrum *3* is not related to line broadening due to the dipole–dipole interaction between adsorbed NO molecules: reducing the amount of adsorbed NO by a factor of 10–20 decreases the intensity of the ESR signal of NO but no hyperfine structure appears [14]. According to earlier data [20], the presence of a hyperfine structure in the ESR spectra of NO adsorbed on CeO_2 and 10%CeO_2/ZrO_2 indicates a weak acidity of the Ce^{4+} ions, while its absence in the ESR spectrum of NO on ZrO_2 suggests that the Zr^{4+} ions are strongly acidic.

The ESR spectra of NO adsorbed on CeO_2, 10%CeO_2/ZrO_2, and ZrO_2 at –196°C are stable and remain unchanged upon pumping of the samples for 1 h. The intensity of the spectra decreases as the samples are heated without pumping. The disappearance of the spectra between –150 and –80°C is accompanied by NO desorption into the sample bulk. Subsequent cooling of the sample to –196°C results in NO adsorption, and the ESR signal of NO is completely recovered.

When oxygen (P = 50 Pa, T = –196°C) is admitted to a $CeO_2(O_2$, T = 400–600°C) sample containing adsorbed NO, the ESR signal of NO disappears and an ESR signal from O_2^- appears ($(1.2–2.5) \times 10^{16}$ m^{-2}), whose spectrum is similar to that presented in Fig. 1. Pumping the sample has no effect on the shape or intensity of the ESR spectrum of O_2^- and does not bring about an ESR spectrum of NO. After subsequent addition of NO, the ESR signal of O_2^- disappears and the ESR signal of NO is completely recovered. After the sample is pumped, adding O_2 results in the disappearance of the ESR signal of NO but no ESR signal of O_2^- appears. The adsorption of NO on the pumped sample again recovers the ESR signal of NO. The reversible recovery and disappearance of the ESR signal of NO during the adsorption of NO and O_2, respectively, without O_2^- formation indicate that the paramagnetic NO adsorption species is not involved in the formation of $O_2^-(NO + O_2)$ on CeO_2. Earlier, we drew a similar conclusion for the adsorption of NO and O_2 on ZrO_2 [14].

On the one hand, the disappearance of the NO signal upon admission of oxygen to the sample is, probably, due to the displacement of NO molecules by oxygen from the surface to the gas phase and the removal of NO by pumping. On the other hand, the interaction of O_2^- with NO on the surface probably produces diamagnetic complexes ($NO–O_2^-$), which are not observed in the ESR spectrum.

The interaction between adsorbed NO and O_2 on 10%$CeO_2/ZrO_2(O_2$, 400°C) at –196°C also results in the disappearance of the signal from NO and in the appearance of the signal presented in Fig. 7 (curve *1*). After the sample is heated to T = 20°C under continuous pumping, spectrum *1* transforms into spectrum *2*, which is due to O_2^-–Zr^{4+}. The subtraction of spectrum *2* from spectrum *1* gives spectrum *3* with g-tensor parameters of $g_1 = 2.036$ and $g_2 = 2.011$, which are characteristic of O_2^- located on Ce^{4+} cations in isolated anionic vacancies. Therefore, at –196°C, $O_2^-(NO + O_2)$ radical anions are formed on the 10%CeO_2/ZrO_2 sample, being stabilized both on particles of the CeO_2 phase and on the surface of the ZrO_2 support.

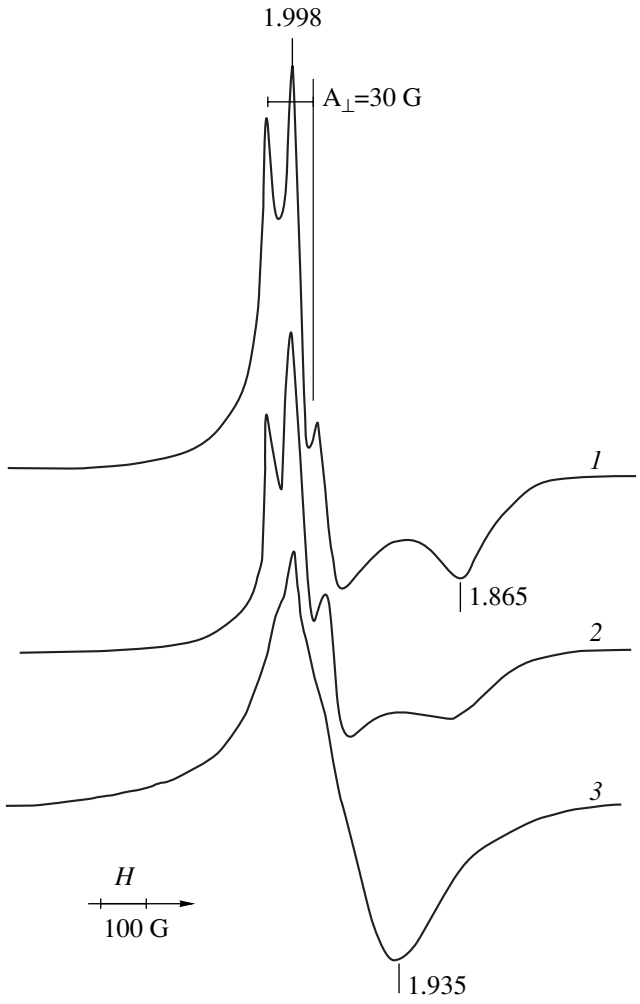

Fig. 6. ESR spectra of NO adsorbed at −196°C on (*1*) $CeO_2(O_2$, 300°C), (*2*) 10%$CeO_2/ZrO_2(O_2$, 500°C), and (*3*) $ZrO_2(O_2$, 500°C).

Because the paramagnetic NO adsorption species is inactive in $O_2^-(NO + O_2)$ formation, NO complexes on CeO_2 were studied by TPD and IR spectroscopy.

IR Spectroscopic Data

The IR spectra of adsorption complexes on $CeO_2(O_2$, 600°C) at 20°C are presented in Fig. 8. These spectra were obtained after NO adsorption followed by pumping of the sample at different temperatures for 10 min. For instance, after NO ($P = 10^3$ Pa) is let in, absorption bands due to N_2O (2241 and 1252 cm^{-1}) and chelates of the nitrite ion NO_2^- (1275, 1166, and 824 cm^{-1}) are observed in the spectrum (curve *1*) [18, 19]. After the sample is pumped at 20°C, the absorption bands of N_2O disappear while those of NO_2^- remain unchanged (curve *2*). Heating the sample in vacuum at 100°C exerts no effect on the spectrum of nitrites

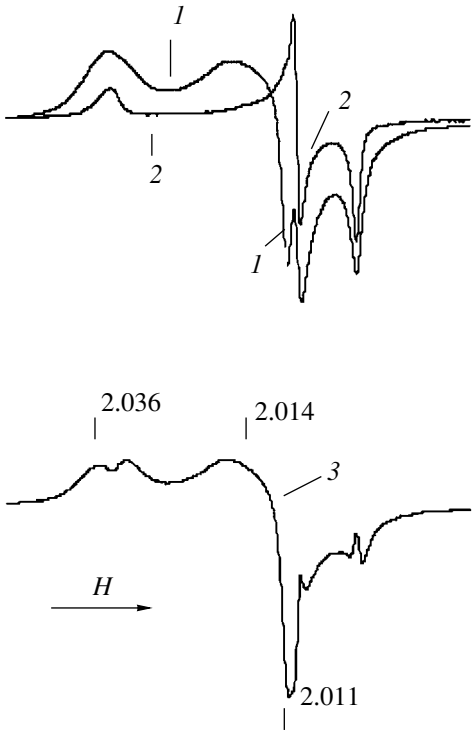

Fig. 7. ESR spectra of 10%CeO_2/ZrO_2(O_2, 500°C) after the (*1*) interaction between adsorbed NO and O_2 at –196°C and (*2*) subsequent pumping at 20°C and cooling to –196°C. (*3*) Differential spectrum obtained by subtracting spectrum *2* from spectrum *1*.

(curve *3*), while heating at 300°C results in the disappearance of the absorption bands of nitrites and in the appearance of absorption bands at 1554, 1222, and 1013 cm^{-1}, assignable to monodentate or bidentate nitrates NO_3^- (curve *4*) [21]. The nitrates decompose in vacuum at 480°C.

TPD Data

Oxygen (curve *1*) and NO (curve *2*) desorption spectra for oxidized CeO_2(O_2, 600°C) are presented in Fig. 9. It follows from the shape of spectrum *1* that, after this specimen is treated with oxygen at 20°C and $P = 2 \times 10^2$ Pa, O_2 is desorbed at $T_{max} = 470$°C. A similar spectrum was recorded when CeO_2(O_2, 600°C) was heated without oxygen treatment. This suggests that at 20°C oxygen does not form stable adsorption species on oxidized CeO_2. The O_2 desorption temperature is equal to the temperature of CeO_2 reduction in vacuum (Fig. 3). The amount of desorbed O_2 converted to surface concentration is $N_{O_2} = 1 \times 10^{17}$ m^{-2} and does not exceed 2% of the amount of O^{2-} ions on the surface. Apparently, O_2 desorption is due to the removal of interstitial oxygen from the Ce^{4+} cations.

Spectrum *2* illustrates the desorption of NO that has been adsorbed at 20°C and $P = 10^3$ Pa. The low-temperature region (40–180°C) contains a peak with two maxima at $T_{max} = 70$ and 100°C ($N_{NO} = 1.2 \times 10^{17}$ m^{-2}). Between 200 and 520°C, there are two peaks at $T_{max} = 260$ and 480°C. The NO concentrations corresponding to these peaks are approximately the same and are equal to 3.3×10^{17} m^{-2}. At 400–520°C, this sample desorbs the same amount of oxygen as the oxidized sample.

It follows from the TPD data that only stable nitrito complexes are formed on the oxidized CeO_2 surface upon NO adsorption at 20°C. Approximately 50% of them decompose with NO desorption at ~300°C, and the other 50% turn into surface nitrates decomposing at ~480°C. The nature of the NO complexes decomposing at 70–100°C remains unclear. They may be the two hypernitrite species that are assumed [19] to be intermediates in the formation of N_2O. The absorption bands due to these hypernitrites (1350, 1015, and 954 cm^{-1} for *cis*-$N_2O_2^{2-}$ and 1105 cm^{-1} for *trans*-$N_2O_2^{2-}$) were not observed (Fig. 8), probably because of the low concentration of these species on the surface.

DISCUSSION

Mechanism of O_2^-(NO + O_2) Formation on Oxidized CeO_2

Oxygen adsorption on CeO_2 that has been reduced in hydrogen or vacuum is known to produce O_2^- radical anions through electron transfer from Ce^{3+} to adsorbed O_2 [17]. Ce^{3+} cations are paramagnetic; however, they are not detected by ESR in the reduced CeO_2 and CeO_2/ZrO_2 samples at –196 and 20°C, probably because of the short time of spin–lattice relaxation. Ce^{3+} cations are also absent from oxidized CeO_2 and CeO_2/ZrO_2 because O_2 adsorption on these materials produces O_2^-. The formation of O_2^-(NO + O_2) on oxidized CeO_2 indicates that NO adsorption complexes are involved in this reaction as electron donors.

Let us consider the mechanism of this reaction in more detail. We believe that active sites in this reaction are coordinately unsaturated ions Ce^{4+} and O^{2-} formed by surface dehydroxylation. This assumption is favored by the fact that the concentration of O_2^-(NO + O_2) increases with increasing CeO_2 oxidation temperature (Fig. 3, curve *1*).

Depending on the NO adsorption temperature, different surface compounds form on the coordinately unsaturated ions Ce^{4+} and O^{2-}: NO–Ce^{4+} (–196°C), nitrites NO_2^-, nitrous oxide N_2O (20°C), and nitrates NO_3^- (300°C). The participation of the compounds NO–Ce^{4+} and NO_3^- in this reaction seems to be improbable for the following reasons. For the first compound, O_2 adsorption at –196°C is accompanied by the decom-

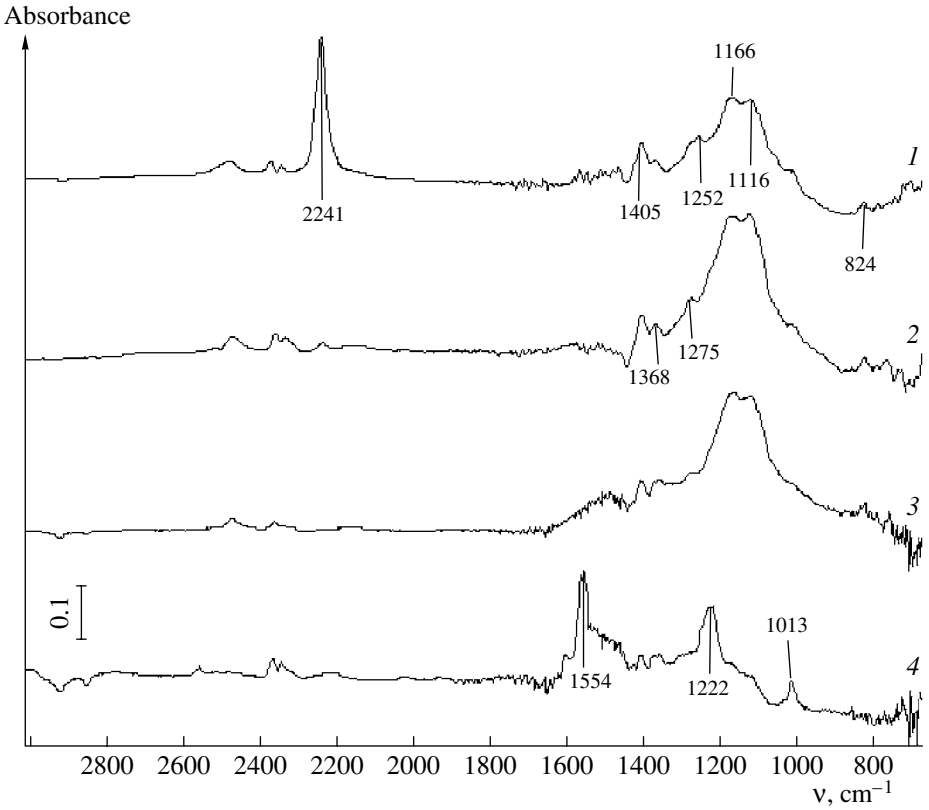

Fig. 8. IR spectra of $CeO_2(O_2, 600°C)$ after (*1*) admission of NO at 20°C and (*2–4*) subsequent pumping at (*2*) 20, (*3*) 100, and (*4*) 300°C.

position of NO–Ce^{4+} and by the displacement of NO into the sample bulk without O_2^- formation. In the second case, nitrates result from nitrites at 300°C, well above the $O_2^-(NO + O_2)$ formation temperature (20°C). Nitrous oxide is inactive in the reaction because no O_2^- results from the coadsorption of N_2O and O_2^- on CeO_2. The appearance of free electrons upon the formation of chelate nitrites seems to be most probable. According to an earlier report [19], chelate nitrite results from interaction between an NO molecule and a coordinately unsaturated ion pair Ce^{4+}–O^{2-} followed by electron transfer from the NO molecule to the surface with reduction of the Ce^{4+} cation to Ce^{3+} (reaction (I)). The reduction of cations upon nitrite formation is indicated by the appearance of electrons in the conduction band [22]. In this case, O_2^- formation is due to adsorbed O_2 molecules capturing electrons from the conduction band (reaction (II)).

$$NO + \overset{\square}{\underset{|}{Ce^{4+}}}\!\!-O^{2-} \Rightarrow \left|\begin{array}{c} N \\ O \quad O \\ Ce^{3+} \end{array}\right|^{-}, \qquad \text{(I)}$$

$$Ce^{3+} + O_2 \Rightarrow Ce^{4+}\!\!-O_2^-. \qquad \text{(II)}$$

Since the ESR spectra of $O_2^-(NO + O_2)$ and $O_2^-(O_2)$ on the oxidized and reduced CeO_2 samples are similar, it is evident that the $O_2^-(NO + O_2)$ species are stabilized in the coordination sphere of Ce^{4+} cations near nitrito

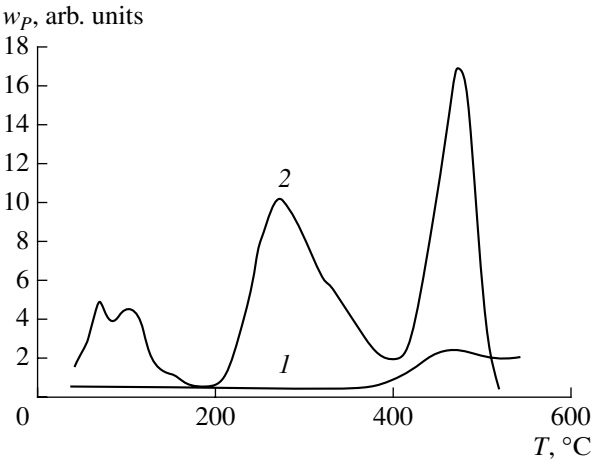

Fig. 9. (*1*) O_2 and (*2*) NO temperature-desorption spectra for $CeO_2(O_2, 600°C)$. Adsorption conditions: 20°C, $P_{O_2} = 2 \times 10^2$ Pa, $P_{NO} = 10^3$ Pa.

complexes. Probably, the formation of $O_2^-(NO + O_2)$ on ZrO_2 proceeds by a similar mechanism [14].

Inhibition of $O_2^-(NO + O_2)$ Formation on ZrO_2 by CeO_2

It was demonstrated [23] that 2 mol % MoO_3 supported on ZrO_2 completely inhibits the formation of $O_2^-(NO + O_2)$ on ZrO_2 through immobilization of Mo^{6+} cations on surface O^{2-} ions. According to the data presented in Fig. 5, this reaction is not completely inhibited by CeO_2 even when the concentration of supported Ce^{4+} ions exceeds the surface concentration of Zr^{4+} cations by a factor of 3, as in the 10%CeO_2/ZrO_2 sample. We believe that the fact that the activity of ZrO_2 decreases as the percentage of supported cerium oxide increases from 0.5 to 2% is due to single cerium oxo complexes and dimeric oxide clusters covering the surface. Further increase in the CeO_2 content from 2 to 10% does not diminish the free surface area of the support, probably because the dimeric cerium oxide clusters transform into trimeric ones. The formation of trimeric clusters (or of the CeO_2 phase on the ZrO_2 surface in the case of 10%CeO_2/ZrO_2) is indicated by the appearance of the hyperfine structure characteristic of NO adsorbed on CeO_2 in the ESR spectrum upon the adsorption of NO (–196°C) (Fig. 6) and by the formation of $O_2^-(NO + O_2)$ on the Ce^{4+} cations of the CeO_2 clusters (Fig. 7). Note that $O_2^-(NO + O_2)$ was observed at –196°C on CeO_2 clusters and at 20°C on a CeO_2 monolith. This difference in O_2^- stabilization temperature can be explained by the strong interaction between the ZrO_2 support and cerium ions in the CeO_2 clusters [24].

On the Nature of the Bonds between O_2^- and Ce^{4+} and between O_2^- and Zr^{4+} and of the Acidity of Cations in CeO_2 and CeO_2/ZrO_2

The bonds between the oxygen radical and the metal ion in the O_2^-–Ce^{4+} and O_2^-–Zr^{4+} complexes differ in nature. For most metal oxides, the g tensor of O_2^- is consistent with the ionic model, according to which the smallest component of the g tensor must be equal to the value of a free electron (g_e) [25]. For the O_2^-–Zr^{4+} complexes, $g_3 = 2.003$, which is close to $g_e = 2.0023$ (Fig. 4), indicating ionic bonding in these compounds. For all O_2^-–Ce^{4+} complexes (Figs. 1, 7), g_3 is higher than g_e, in agreement with the ionic model. In this case, the bond is covalent rather than ionic. This covalent bond results from the overlap of the occupied π_y orbital of oxygen and unoccupied 4*f* orbitals of the cerium cation [24].

The covalent bond in the O_2^-–Ce^{4+} complexes is weaker than the ionic bond in the O_2^-–Zr^{4+} complexes: the O_2^-–Ce^{4+} complexes decompose below 50°C, whereas the O_2^-–Zr^{4+} complexes decompose at 270°C. In this case, we can assume that Zr^{4+} cations are more acidic than Ce^{4+} cations. This assumption is also suggested by the analysis of the hyperfine structures of the ESR spectra of NO adsorbed on CeO_2 and ZrO_2 at –196°C (Fig. 6).

REFERENCES

1. Shelef, M. and Graham, G.M., *Catal. Rev.*, 1994, vol. 36, p. 433.
2. Balducci, G., Kaspar, J., Fornasiero, P., Graziani, M., Islam, M.S., and Gale, J.D., *J. Phys. Chem. B*, 1997, vol. 101, p. 1750.
3. Balducci, G., Kaspar, J., Fornasiero, P., Graziani, M., and Islam, M.S., *J. Phys. Chem. B*, 1998, vol. 102, p. 557.
4. Fornasiero, P., Balducci, G., Monte, R.Di., Kaspar, J., Sergo, V., Gubitosa, G., Ferrero, A., and Graziani, M., *J. Catal.*, 1996, vol. 164, p. 173.
5. Hori, C.E., Permana, H., Brenner, Y., Rahmoeller, K.M., and Belton, D.N., *Apll. Catal., B*, 1998, vol. 16, p. 105.
6. Daturi, M., Bion, N., Saussey, J., Lavalley, J.-C., Hedouin, C., Seguelong, T., and Blanchard, G., *Phys. Chem. Chem. Phys.*, 2001, vol. 3, p. 252.
7. Giamello, E., *Catal. Today*, 1998, vol. 41, p. 239.
8. Cordischi, D., Indoviva, V., and Occhiuzzi, M., *J. Chem. Soc., Faraday Trans.*, 1978, vol. 74, no. 1, p. 456.
9. Ito, T., Yoshioka, M., and Nouda, T., *J. Chem. Soc., Faraday Trans.*, 1983, vol. 79, no. 10, p. 2277.
10. Garrone, G., Giomello, E., Ferraris, M., and Spoto, G., *J. Chem. Soc., Faraday Trans.*, 1992, vol. 88, no. 3, p. 333.
11. Ito, T., Watanabo, T., Tashiro, T., and Toi, K., *J. Chem. Soc., Faraday Trans.*, 1989, vol. 85, no. 8, p. 2381.
12. Krylov, O.V., *Kinet. Katal.*, 1973, vol. 14, no. 1, p. 35.
13. Konin, G.A., Il'ichev, A.N., Matyshak, V.A., and Korchak, V.N., *Mendeleev Commun.*, 2000, no. 5, p. 197.
14. Il'ichev, A.N., Konin, G.A., Matyshak, V.A., Kulizade, A.M., Korchak, V.N., and Yan, Yu.B., *Kinet. Katal.*, 2002, vol. 43, no. 2, p. 235.
15. Tret'yakov, I.I., Shub, B.R., and Sklyarov, A.V., *Zh. Fiz. Khim.*, 1970, vol. 44, p. 2112.
16. *Handbuch der preparativen anorganischen Chemie*, von Brauer, G., Ed., Stuttgart: Ferdinand Enke, 1981.

17. Soria, J., Martinez-Arias, A., and Conesa, J.C., *J. Chem. Soc., Faraday Trans.*, 1995, vol. 91, no. 11, p. 1669.

18. Niwa, M., Furukawa, Y., and Murakami, Y., *J. Colloid Interface Sci.*, 1982, vol. 86, no. 1, p. 260.

19. Martinez-Arias, A., Soria, J., Conesa, J.C., Seoane, X.L., Arcoya, A., and Catalune, R., *J. Chem. Soc., Faraday Trans.*, 1995, vol. 91, no. 11, p. 1679.

20. Rudolf, T., Bohlmann, W., and Poppl, A., *J. Magn. Reson.*, 2002, vol. 155, p. 45.

21. Hadgiivanov, K.I., *Catal. Rev.*, 2000, vol. 42, nos. 1–2, p. 71.

22. Vol'kinshtein, F.F., *Fiziko-khimiya poverkhnosti poluprovodnikov* (Physical Chemistry of the Semiconductor Surface), Moscow: Nauka, 1973.

23. Il'ichev, A.N., Shibanova, M.D., and Korchak, V.N., *Kinet. Katal.*, 2004, vol. 45, no. 1, p. 126.

24. Soria, J., Coronado, J.M., and Conesa, J.C., *J. Chem. Soc., Faraday Trans.*, 1996, vol. 92, no. 9, p. 619.

25. Che, M. and Tench, A.J., *Adv. Catal.*, 1983, vol. 32, p. 1.